TOC1 in Nicotiana attenuata regulates efficient allocation of nitrogen to defense metabolites under herbivory stress

Valim, Henrique ; Dalton, Heidi ; Joo, Youngsung ; McGale, Erica ; Halitschke, Rayko ; Gaquerel, Emmanuel ; Baldwin, Ian T ; Schuman, Meredith Christine

Abstract: The circadian clock contextualizes plant responses to environmental signals. Plants use temporal information to respond to herbivory, but many of the functional roles of circadian clock components in these responses, and their contribution to fitness, remain unknown. We investigate the role of the central clock regulator TIMING OF CAB EXPRESSION 1 (TOC1) in Nicotiana attenuata's defense responses to the specialist herbivore Manduca sexta under both field and glasshouse conditions. We utilize 15N pulse-labeling to quantify nitrogen incorporation into pools of three defense compounds: caffeoylputrescine (CP), dicaffeoyl spermidine (DCS) and nicotine. Nitrogen incorporation was decreased in CP and DCS and increased in nicotine pools in irTOC1 plants compared to empty vector (EV) under control conditions, but these differences were abolished after simulated herbivory. Differences between EV and irTOC1 plants in nicotine, but not phenolamide production, were abolished by treatment with the ethylene agonist 1-methylcyclopropene. Using micrografting, TOC1's effect on nicotine was isolated to the root and did not affect the fitness of heterografts under field conditions. These results suggest that the circadian clock contributes to plant fitness by balancing production of metabolically expensive nitrogen-rich defense compounds and mediating the allocation of resources between vegetative biomass and reproduction.

DOI: https://doi.org/10.1111/nph.16784

New Phytologist

Research

TOC1 in *Nicotiana attenuata* regulates efficient allocation of nitrogen to defense metabolites under herbivory stress

Henrique Valim[1], Heidi Dalton[1], Youngsung Joo[1], Erica McGale[1], Rayko Halitschke[1], Emmanuel Gaquerel[1,2], Ian T. Baldwin[1] and Meredith C. Schuman[1,3]

[1]Department of Molecular Ecology, Max Planck Institute for Chemical Ecology, Hans-Knöll-Straße 8, Jena 07745, Germany; [2]Institute of Plant Molecular Biology, University of Strasbourg, 12 Rue du Général Zimmer, Strasbourg 67084, France; [3]Department of Geography & Department of Chemistry, University of Zurich, Winterthurerstrasse 190, Zurich 8057, Switzerland

Authors for correspondence:
Ian T. Baldwin
Tel: +49 3641571100
Email: baldwin@ice.mpg.de

Meredith C. Schuman
Tel: +49 15759161261
Email: meredithchristine.schuman@uzh.ch

Received: *18 May 2020*
Accepted: *16 June 2020*

New Phytologist (2020)
doi: 10.1111/nph.16784

Key words: ethylene signaling, herbivory, *Nicotiana attenuata*, nitrogen allocation, TIMING OF CAB EXPRESSION1.

Summary

- The circadian clock contextualizes plant responses to environmental signals. Plants use temporal information to respond to herbivory, but many of the functional roles of circadian clock components in these responses, and their contribution to fitness, remain unknown.
- We investigate the role of the central clock regulator TIMING OF CAB EXPRESSION 1 (TOC1) in *Nicotiana attenuata*'s defense responses to the specialist herbivore *Manduca sexta* under both field and glasshouse conditions. We utilize ^{15}N pulse-labeling to quantify nitrogen incorporation into pools of three defense compounds: caffeoylputrescine (CP), dicaffeoyl spermidine (DCS) and nicotine.
- Nitrogen incorporation was decreased in CP and DCS and increased in nicotine pools in irTOC1 plants compared to empty vector (EV) under control conditions, but these differences were abolished after simulated herbivory. Differences between EV and irTOC1 plants in nicotine, but not phenolamide production, were abolished by treatment with the ethylene agonist 1-methylcyclopropene. Using micrografting, *TOC1*'s effect on nicotine was isolated to the root and did not affect the fitness of heterografts under field conditions.
- These results suggest that the circadian clock contributes to plant fitness by balancing production of metabolically expensive nitrogen-rich defense compounds and mediating the allocation of resources between vegetative biomass and reproduction.

Introduction

Because they are both sessile organisms and at the base of most food chains, plants are under strong pressure to produce effective defenses in the face of mobile herbivores. Several theories have been developed in an attempt to quantify plant defense responses as a function of different factors, in order to explain and predict patterns observed under natural conditions, with varying degrees of success (see Schuman & Baldwin, 2016). Many of these theories attempt to determine trade-offs between growth and defense (Herms & Mattson, 1992), both of which depend on the same limited resources (Bryant *et al.*, 1983; Chapin *et al.*, 1990) and can be alternatively prioritized among plant tissues with different fitness values (McKey, 1974, 1979; Rhoades, 1979). Generating testable predictions from these theories has proven challenging largely because they address different levels of analysis, from mechanism to function (Tinbergen, 1963; Sherman, 1988), and the proposed mechanisms are not grounded in plant physiology. Furthermore, most plant defense theories do not consider the definition of defense as the contribution of a trait to the Darwinian fitness of plants under attack (Karban & Baldwin, 1997; Stamp, 2003; Massad *et al.*, 2012; Schuman & Baldwin, 2016).

One component is the importance of timing to the function of plant defense. Herbivory occurs unpredictably over a plant's lifetime, and plant defense responses are highly plastic and often elicited by herbivory (Lynds & Baldwin, 1998; Wu & Baldwin, 2010; Meldau *et al.*, 2012; Wagner & Mitchell-Olds, 2018). Herbivore feeding behavior can be diurnally rhythmic, while plant defenses are likely constrained by the circadian clock in order to maximize resource use (Goodspeed *et al.*, 2012, 2013b). The plant circadian clock is an endogenous mechanism that touches upon nearly every aspect of plant metabolism (Greenham & McClung, 2015; Nohales & Kay, 2016; Sanchez & Kay, 2016). As such, individual components of the clock have been shown to modulate responses to a variety of external stimuli and stresses, including herbivory (Takase *et al.*, 2013; Seo & Mas, 2015; Sharma & Bhatt, 2015; Joo *et al.*, 2018; Zhang *et al.*, 2019).

Despite evidence for the clock's role in modulating responses, few studies have adressed its significance for maintaining plant fitness in natural, diurnal environments. The circadian clock component GIGANTEA (GI) maximizes the fitness of *Oryza sativa* sown at variable times under field conditions (Izawa *et al.*, 2011; Izawa, 2012), while the central circadian clock component

TIMING OF CAB EXPRESSION 1 (TOC1), which modulates a variety of growth and stress responses (Somers *et al.*, 1998; Legnaioli *et al.*, 2009; Soy *et al.*, 2016; Zhu *et al.*, 2016), enhances fitness during drought stress in the field (Valim *et al.*, 2019). Although there have been few studies tying clock components to fitness outcomes under biotic stress, the clock is known to regulate responses to herbivory. Basal levels of the phytohormone jasmonic acid (JA), which is involved in regulating downstream responses to biotic stresses, are under circadian regulation in Arabidopsis (Goodspeed *et al.*, 2013a). Jasmonic-acid-induced responses to herbivory are known to be under diurnal regulation in other plant species, with darkness affecting JA accumulation. However, whether JA accumulation is under circadian regulation remains unknown (see e.g. *Phaseolus lutatus*; Arimura *et al.*, 2008). In the desert annual *Nicotiana attenuata*, performance of the herbivore *Manduca sexta* is similarly dominated by diurnal rather than circadian patterns (Herden *et al.*, 2016), and several JA-induced secondary metabolites are under diurnal regulation (Halitschke *et al.*, 2000; Kim *et al.*, 2011; Gulati *et al.*, 2014; Joo *et al.*, 2018). However, the clock component Zeitlupe (ZTL) does regulate the JA-mediated induction of nicotine in *N. attenuata* (Li *et al.*, 2018).

Jasmonic-acid-induced herbivory responses can be specific and are mediated by interactions with other phytohormone pathways. In the wild tobacco species *Nicotiana sylvestris* and *N. attenuata*, oral secretions of *M. sexta* dampen the JA-elicited increase in nicotine observed after elicitation with mechanical wounding or the application of exogenous JA (McCloud & Baldwin, 1997; Kahl *et al.*, 2000). Fatty acid–amino acid conjugates (FACs) in the oral secretions of *M. sexta* are necessary and sufficient to dampen this nicotine response, and function by eliciting an ethylene burst (Kahl *et al.*, 2000; Halitschke *et al.*, 2001; Von Dahl *et al.*, 2007). Ethylene signaling suppresses JA-induced nicotine production in *Nicotiana* spp. by suppressing expression of *ethylene response factor* (*ERF*) transcription factors that bind to the promoter regions of nicotine biosynthesis genes such as *putrescine N-methyltransferase* (PMT), and the ethylene burst leads to large-scale reconfiguration of transcriptomic responses to herbivory (Shoji *et al.*, 2000, 2010; Voelckel & Baldwin, 2004). Ethylene responses are under circadian regulation in Arabidopsis, and *TOC1* silencing alters the rhythmicity of ethylene emissions (Thain *et al.*, 2004). Nonetheless, it is unknown whether any functional benefits of rhythmic ethylene emissions are directly mediated by the circadian clock.

Although nicotine provides *Nicotiana* spp. with a potent defense in nature (Steppuhn *et al.*, 2004), plants elicited by the nicotine-tolerant specialist *M. sexta* do not increase nicotine production, and subsequently experience lower fitness costs of elicitation than plants elicited by exogenous JA treatments or when ethylene signaling is blocked, leading to high nicotine accumulation after elicitation (Voelckel *et al.*, 2001). This may be because plants mobilize their limited resources to more effective defenses, given nicotine's high metabolic cost, and/or because nicotine may be co-opted by *M. sexta* larvae as a defense against parasitism and predation (Thorpe & Barbosa, 1986; Baldwin & Ohnmeiss, 1994; Kumar *et al.*, 2014). *Nicotiana attenuata* contains many secondary metabolites of defensive value, with the phenolamides caffeoylputrescine (CP) and dicaffeoyl spermidine (DCS) effectively limiting *M. sexta* performance (Kaur *et al.*, 2010). CP and DCS are highly abundant in *M. sexta*-elicited plants and are correlated with elicited jasmonyl isoleucine (JA-Ile) contents in leaves of natural accessions (Gaquerel *et al.*, 2014).

Transcriptional activation of *MYB8*, the key regulator of phenolamide biosynthesis, requires functioning JA signaling (Onkokesung *et al.*, 2012). Silencing *MYC2*, the primary transcription factor at the interface of JA biosynthesis and downstream signaling, does not lead to decreases in CP and DCS after elicitation, suggesting an alternate JA-induced pathway independent of the COI1-mediated JAZ/MYC2 module that regulates nicotine biosynthesis (Chini *et al.*, 2007; Thines *et al.*, 2007; Sheard *et al.*, 2010; Woldemariam *et al.*, 2013). Nicotine biosynthesis is also directly regulated by an interaction between the circadian clock component ZTL and a JAZ/MYC2 module independently of COI1, while phenolamide levels are not strongly affected by silencing *ZTL* (Li *et al.*, 2018). Phenolamides and nicotine are nitrogen (N)-rich and thus presumably metabolically expensive secondary metabolites, and efficient maintenance of *N. attenuata*'s N composition is critical to its survival in environments characterized by high intraspecific competition (Baldwin *et al.*, 1998; Lynds & Baldwin, 1998; Ullmann-Zeunert *et al.*, 2012, 2013). Thus, we sought to examine the role of the circadian clock in the regulation of these defense metabolites at the intersection of JA and ethylene signaling, in addition to examining the implications of this role on plant fitness under field conditions by abrogating *TOC1* expression.

Abrogating *TOC1* expression via RNAi-mediated silencing leads to broad changes in plant responses to simulated herbivory. We observed that *TOC1* silencing leads to delays in jasmonate-dependent signaling after elicitation with *M. sexta* oral secretions, consistent with previous findings linking the circadian clock component *ZTL* to the jasmonate-mediated regulation of nicotine biosynthesis in *N. attenuata*. Interestingly, we also observed significant decreases in production of CP and DCS, and increased rather than decreased nicotine production. We performed ^{15}N pulse labeling experiments to ask whether N incorporation into phenolamide and nicotine pools is changed by elicitation, and observed that N introduced as $^{15}NO_3^-$ is preferentially incorporated into nicotine pools under control conditions in irTOC1 plants, while allocation becomes equally distributed between phenolamides and nicotine after elicitation with *M. sexta* oral secretions. These findings are consistent with previous evidence that herbivory disrupts the rhythmicity of the clock (Joo *et al.*, 2018), and that nicotine pools in other *Nicotiana* species are homeostatic and do not function as sources of N (Baldwin & Ohnmeiss, 1994; Ohnmeiss & Baldwin, 1994).

Because irTOC1 plants overproduce nicotine, contrary to the phenotype which would be predicted by comparison with irZTL plants, we asked whether ethylene signaling may be compromised in irTOC1 plants. Although the ethylene burst is not different in irTOC1 plants, differences between empty vector (EV) and irTOC1 plants in nicotine production are abolished by treatment with 1-methylcyclopropene, an ethylene signaling receptor

blocker, pointing to an attenuation of the ethylene signaling feedback loop (Von Dahl *et al.*, 2007). This effect was specific to nicotine, as differences in phenolamide accumulation remained largely unchanged. Finally, we find that restoring *TOC1* function in shoots, but not in roots, via a seedling micrografting approach is sufficient to decouple differential phenolamide and nicotine accumulation and the fitness disadvantages of whole-plant irTOC1 silencing under field conditions, leading to plants with high levels of N-rich defense compounds and uncompromised fitness relative to EV plants. These results indicate tissue-specific roles for *TOC1* in the production of metabolically expensive N-rich defense compounds via an interplay between JA and ethylene signaling.

Materials and Methods

Plant materials and constructs

Lines were derived from seeds originally collected from natural populations of *Nicotiana attenuata* Torr. ex S. Watson from the Desert Inn Ranch near Santa Clara, UT, USA (Baldwin *et al.*, 1994). Seed germination and plant growth in the glasshouse were carried out as described by Krügel *et al.* (2002) and undertaken in a glasshouse in Jena, Germany, under a 16 h : 8 h, light : dark photoperiod. Screening of the EV line (pSOL3NC, line no. A-04-266-3) for a single homozygous transgene insertion and absence of off-target effects is described by Bubner *et al.* (2006). Screening of TOC1-silenced (ir) lines (pSOL8_16844, A-11-205-4) via RNAi is described by Yon *et al.* (2012), with additional screening described in Valim *et al.* (2019). Unless specified in figure captions, the irTOC1-205 line was used for all experiments described in this study. Importation and release of transgenic plants were carried out under Animal and Plant Health Inspection Service (APHIS) import permit nos. 07-341-101n (EV) and 11-350-102m (irTOC1) and release permit no. 16-013-102r. Field growth conditions were described by McGale *et al.* (2018). Briefly, seedlings were germinated on Gamborg's B5 media (Duchefa, Harleem, the Netherlands) under illumination from fluorescent lights with a 16 h : 8 h, light : dark photoperiod (GE Plant & Aquarium 40 W and GE Warm White 18 W, Cleveland, OH, USA) at ambient temperatures at the field station. One week after germination, seedlings were grafted (see section 2.3, *Micrografting*, below, and Fragoso *et al.* (2011). One to two weeks after grafting, seedlings with four visible leaves were transferred into previously hydrated 50-mm peat pellets (Jiffy 703; Jiffy Products of America Inc., Lorain, OH, USA) treated with borax (sodium tetraborate; Sigma-Aldrich Chemie Gmbh, Munich, Germany) to provide boron, an essential micronutrient (1 : 100 dilution of a 1.1 $g\,l^{-1}$ stock solution), and adapted over 2 wk to the field conditions of high light intensity (over 2.0 $mmol\,m^{-2}\,s^{-1}$ of photosynthetically active radiation; see Joo *et al.*, 2017) and low relative humidity (often 8% relative air humidity during the day during planting; see Nicotiana Attenuata Data Hub: http://nadh.ice.mpg.de/NaDH/fielddata/weather) by keeping seedlings first in shaded, closed translucent plastic 34-quart boxes (Sterilite, Townsend, MA, USA), then opening the boxes, and subsequently transferring open boxes to partial sunlight in mesh tents (Tatonka, Dasing, Germany). Adapted size-matched seedlings were transplanted into an irrigated field plot at the Lytle Ranch Preserve, Santa Clara, Utah, in April 2016, and fitness correlates and biomass were counted at harvest in June 2016.

Simulated herbivory treatments

Manduca sexta L. oral secretions (OS) were collected as described in Voelckel *et al.* (2001). Briefly, larvae were reared from eggs on *N. attenuata* plants, and OS from 3rd- to 5th-instar larvae were collected with gentle vacuum suction and stored under argon at –80°C. *Manduca sexta* feeding was simulated by applying 20 µl of eliciting solution of 1 : 5 (v/v) water-diluted oral secretions immediately to fresh leaf wounds (W + OS) generated by three lines of pattern wheel punctures on either side of a leaf and gently dispersed across the leaf surface with a gloved finger. Plants were elicited during the rosette stage, 10–13 d after potting, and between 13:00 h and 14:00 h.

Micrografting

Seven-day-old seedlings were micro-grafted as described by Fragoso *et al.* (2011). EV (E) and irTOC1 (T) genotypes were used as scions or rootstocks yielding EE, TT, and ET grafts – where the first letter refers to the scion genotype and the second letter to the genotype of the rootstock.

Transcript abundance

Leaf (150 mg) or root tissues (300 mg) were harvested, and RNA was extracted with TRIzol reagent (Invitrogen) according to the manufacturer's instructions. Total RNA was quantified using a NanoDrop (Thermo Scientific, Wilmington, DE, USA) and cDNA was synthesized from 500 ng of total RNA using RevertAid H Minus reverse transcriptase (Fermentas, Vilnius, Lithuania) and oligo (dT) primer (Fermentas). Reverse transcription quantitative PCR (RT-qPCR) was performed in an Mx3005P PCR cycler (Stratagene, San Diego, CA, USA) using SYBR GREEN1 kit (Eurogentec, Liège, Belgium). The *N. attenuata Translation initiation factor 5a-2 (IF5a-2)* gene and the *N. attenuata elongation factor 1a (EF1a)* were used as reference genes for normalization, with *IF5a-2* being used in the experiment represented in Supporting Information Fig. S2 (see Results section on 'Blocking ethylene signaling'), and *EF1a* being used in the experiment represented in Fig. 1. *EF1a* is utilized as a standard reference gene for time series analyses in *N. attenuata*, while the data in Fig. S2 were collected as part of an experiment that involved roots and shoots; for these analyses, *IF51a*, which remains consistent across tissue types in *N. attenuata*, was utilized as a reference gene. The sequences of primers used for RT-qPCR are provided in Table S1. All qRT-PCR data were normalized using the delta-Ct method.

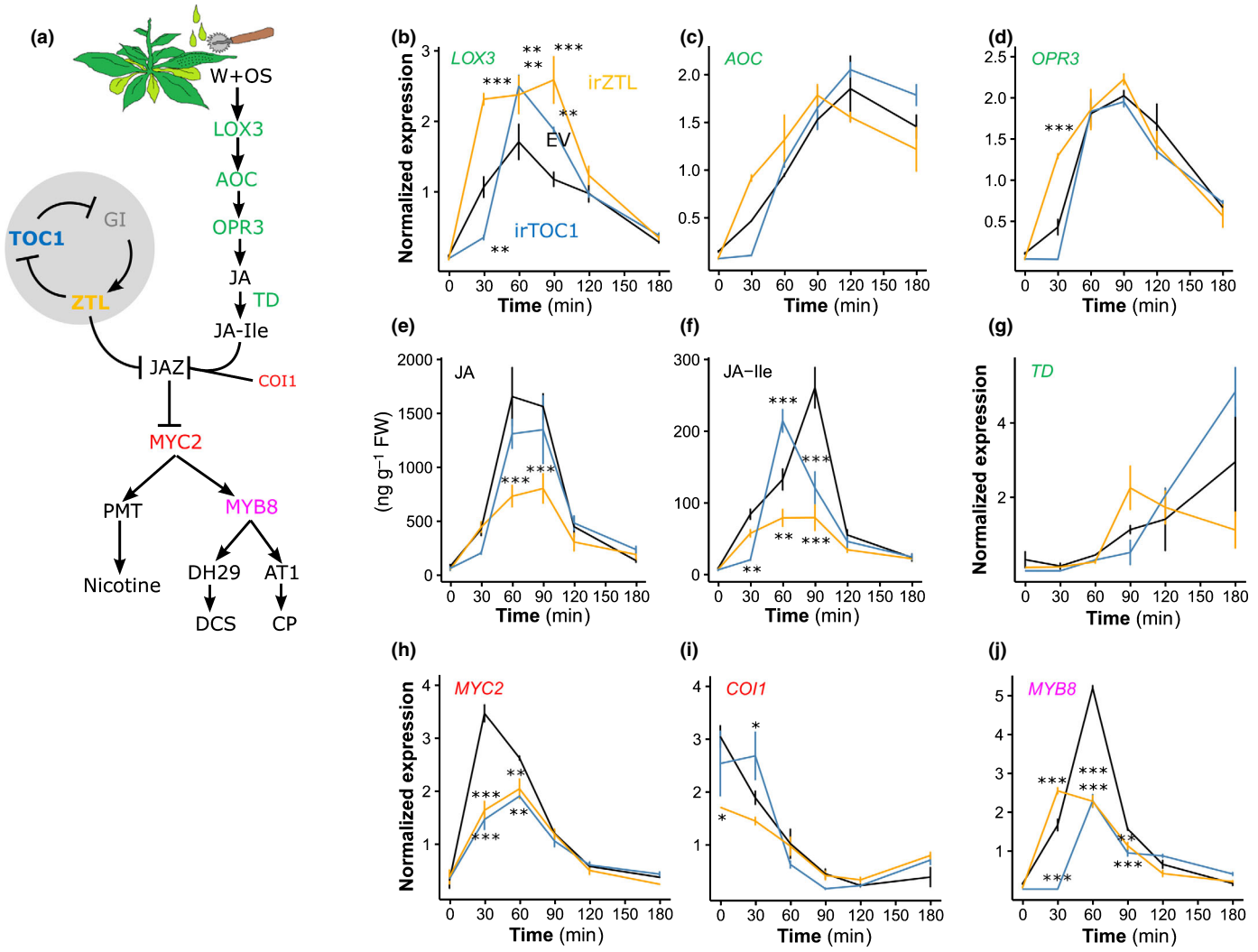

Fig. 1 *TOC1* silencing in *Nicotiana attenuata* leads to a shift in jasmonyl isoleucine (JA-Ile) peak accumulation, delays in jasmonic acid (JA) signaling, and reduced peaks of defense-related transcripts after elicitation with *Manduca sexta* oral secretions. (a) Key biosynthetic and regulatory steps in JA signaling and the effects of *TOC1*-silencing on transcript accumulation in response to elicitation by *M. sexta* oral secretions (W + OS). W + OS-induced transcript accumulation of genes related to (b–d) jasmonate biosynthesis, (e–f) JA and JA-Ile phytohormone levels, and (g–j) transcript levels of downstream signaling genes were analyzed at the indicated time points after the treatment of irTOC1, irZTL, and empty vector (EV) control plants. For all panels, $n = 3$ per genotype and timepoint, and mean ± SE are shown. Data in boxes refer to results of ANOVA tests; asterisks represent significance to EV extracted using Tukey-adjusted pairwise contrasts, within one timepoint: *, $P < 0.05$; **, $P < 0.01$; ***, $P < 0.001$. *GI*, *GIGANTEA*; *TOC1*, *TIMING OF CAB EXPRESSION 1*; *ZTL*, *ZEITLUPE*; *LOX3*, *LIPOXYGENASE3*; *AOC*, *ALLENE OXIDE CYCLASE*; *OPR3*, *12-OXOPHYTODIENOATE REDUCTASE3*, *TD*, *THREONINE DEAMINASE*, *COI1*, *CORONATINE-INSENSITIVE1*.

^{15}N-labeling treatment

To minimize the influence of phenology, irTOC1 plants were germinated 1 wk before EV plants, as they display a delay in flowering of 1 wk (Yon *et al.*, 2012; Valim *et al.*, 2019). After potting, plants did not receive additional fertilizer for 10 d, after which rosette-stage plants were pulse labelled with 5.1 mg of ^{15}N isotope administered as $K^{15}NO_3$ 3 d before W + OS elicitation. Following ^{15}N pulse labeling, plants were watered with an unlabeled nutrient solution every day. Incorporation of ^{15}N into N-containing metabolites was determined as described by Ullmann-Zeunert *et al.* (2012, 2013). Briefly, secondary metabolites were extracted in pre-cooled acidified methanol, and analysis was performed using an electrospray ionization-time of flight mass spectrometer (Bruker Daltonic, Bremen, Germany) as described previously by Gaquerel *et al.* (2010). Average mass spectra were extracted and ^{15}N-incorporation analysis was performed using the Excel spreadsheet ProSIPQuant (Taubert *et al.*, 2011), modified for small metabolites based on compound sum formulae.

1-methylcyclopropene treatment

To minimize the influence of phenology, irTOC1 plants were germinated 1 wk before EV plants (Yon *et al.*, 2012; Valim *et al.*, 2019). Twelve days after potting, plants were pre-exposed for 8 h overnight (22:00 h until 06:00 h) to 1-methylcyclopropene (1-

MCP) and then re-acclimated to glasshouse conditions for 7 h before W + OS elicitation at 13:00 h. Plants (five total) along with the activated solution of 1-MCP were placed within growth chambers fitted with Plexiglas lids and a 14.5 cm fan for air circulation. Following Kahl *et al.* (2000), 500 mg of Ethylblock (0.43% 1-MCP (van der Sprong, Postbus, the Netherlands)) was dissolved in a vial containing 50 ml of alkaline solution (0.75% KOH + NaOH in a 1 : 1 ratio) to release the active substance, 1-MCP, and immediately placed within the chamber. To control for any potential stress responses associated with confinement in chambers and exposure to the solution, control plants were kept in identical chambers supplied with an equivalent amount of alkaline solution.

Phytohormone and secondary metabolite extraction and quantification

Phytohormone analysis of leaf material was performed by ultra performance liquid chromatography–mass spectrometry (EvoQ Elite Triple quad-MS; Bruker Daltonik GmbH, Bremen, Germany) following extraction in pre-cooled acidified methanol and column purification as described by Schäfer *et al.* (2016). Secondary metabolites were extracted similarly in pre-cooled acidified methanol, and analysis was performed by an electrospray ionization-time of flight mass spectrometer (Bruker Daltonik) as described previously by Li *et al.* (2017, 2018).

Statistical analyses

All data were analyzed using R v.3.4.2 (R Core Team, 2018) and RSTUDIO v.1.0.153 (RstudioTeam, 2016). After fitting the data to a linear model, the model residuals were graphically examined for homoscedasticity and normality, and potential outliers were indicated based on Cook's distance as well as a Cook's distance vs leverage analysis (Cook & Weisberg, 1982). Points that were considered highly divergent from the model, based on a cutoff of 0.3 for Cook's distance (Cook's *Di* of observation *i*) as well as above *Di* of 1 for Cook's distance vs leverage, were further investigated to identify any divergent phenotypes, such as unhealthy or dying plants, divergent developmental characteristics, or else inconclusive data processing results, such as poorly separated or missing peaks in the secondary metabolite analysis. Details regarding which outliers were removed, as well as further details of statistical analyses for each dataset, are given in Notes S1.

Pairwise *post-hoc* comparisons were made using the R package EMMEANS (Lenth *et al.*, 2018) using Tukey HSD tests after significant results were observed in a two-way ANOVA. When a two-way ANOVA revealed significance in only one factor, and not in the interaction, the interaction was excluded from the model and the pairwise comparisons were extracted within the nonsignificant factor by performing pairwise *t*-tests. All ANOVAs and relevant contrasts are presented in Notes S1. For regression analyses, estimates of the slopes of the covariate trends were generated for each level of the factor using the function *emtrends* in the R package EMMEANS (Lenth *et al.*, 2018).

Results

TOC1 silencing in *N. attenuata* leads to a shift in JA signaling, and abundance of defense-related gene transcripts after simulated herbivory

ZTL and TOC1 interact directly within the circadian clock (Más *et al.*, 2003; Yon *et al.*, 2012), and silencing ZTL has been shown to decrease nicotine but not phenolamide levels in *N. attenuata* in a JA-independent manner after elicitation with oral secretions from the generalist herbivore *Spodoptera littoralis* (Li *et al.*, 2018). We therefore investigated whether these phenotypes were similar under simulated herbivory after elicitation with oral secretions of a nicotine-tolerant specialist herbivore, *M. sexta*. Transcript abundance of JA biosynthetic genes was not strongly affected by either *ZTL* or *TOC1* silencing (Fig. 1a–d), while JA and JA-Ile concentrations were strongly reduced in *ZTL*-silenced plants only (Fig. 1e,f). Although the peak of JA-Ile induction was shifted in irTOC1 plants, we did not observe a significant change in irTOC1 or irZTL relative to EV in transcript levels of *Threonine Deaminase*, which is strongly elicited by herbivory and contributes to the conversion of threonine into isoleucine, a necessary step in the production of bioactive JA-Ile (see Kang *et al.*, 2006). irTOC1 *TD* transcript abundance was 50% higher than irZTL transcript abundance by 180 min after induction, after JA and JA-Ile concentrations had already decreased (Fig. 1g). The peak of transcript abundance following simulated herbivory was significantly decreased in both irTOC1 and irZTL plants for *MYC2* and *MYB8*, two important coordinators of defense responses following herbivory (Fig. 1h,j), while basal transcript abundance of *COI1* was reduced in *ZTL*-silenced plants only (Fig. 1i).

Silencing *TOC1* leads to increases in nicotine accumulation and decreases in accumulation of both constitutive and inducible phenolamides after simulated herbivory

Given the dampened elicitation of MYC2 and MYB8 in both irTOC1 and irZTL plants, we examined the concentrations of three of *N. attenuata*'s most abundant secondary metabolites, the alkaloid nicotine and the two phenolamides caffeoylputrescine (CP) and dicaffeoyl spermidine (DCS). Nicotine, the signature compound of *Nicotiana* spp., functions as both a constitutive and elicited defense, but is not elicited by oral secretions of the specialist herbivore *M. sexta* (Baldwin *et al.*, 1997; McCloud & Baldwin, 1997; Halitschke *et al.*, 2001). While CP and DCS are both phenolamides, CP is strongly elicited by *M. sexta*herbivory, while DCS is produced constitutively in the plant (Kaur *et al.*, 2010). All three compounds are N-rich and share the precursor molecule putrescine, which is produced as part of the urea cycle (Fig. 2a).

Under control conditions, CP and nicotine levels did not differ significantly among irZTL, irTOC1 and EV plants. At 72 h after induction (hai), irZTL levels of nicotine and CP were similar to the levels reported in Li *et al.* (2018), with a 50% decrease in nicotine accumulation and a nonsignificant tendency towards lower levels of CP compared to EV plants (Fig. 2b,d). irTOC1 levels of nicotine were 45% higher and CP levels were 55% lower compared to EV plants 72 hai (Fig. 2b,d). CP levels were not significantly different

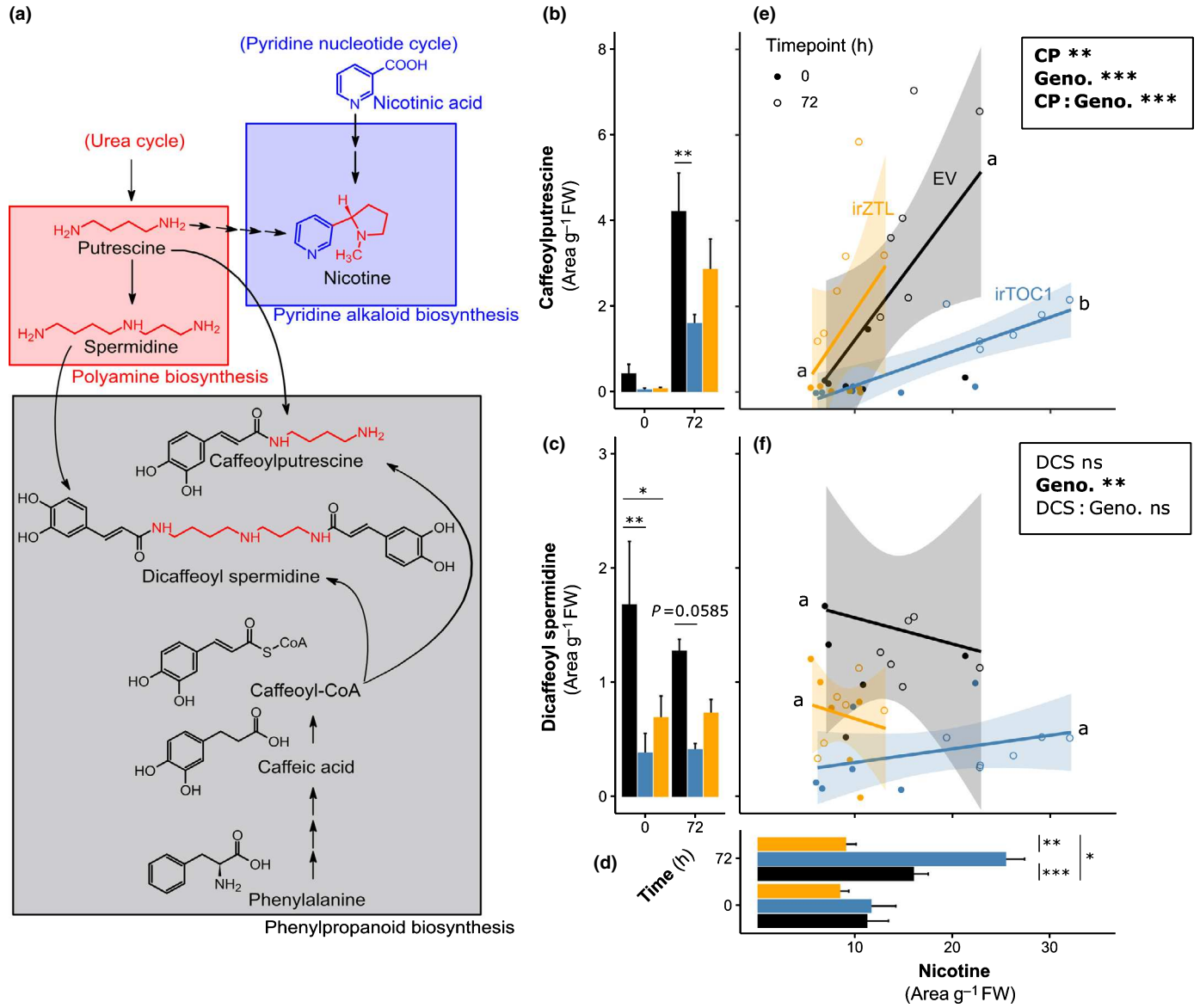

Fig. 2 Silencing *TOC1* changes the ratio between nicotine and phenolamides. (a) Schematic representation of the biosynthetic pathways linking nicotine and caffeoyl-based amines. The relationships between the herbivore-induced (b) phenolamide caffeoylputrescine or the constitutive (c) dicaffeoyl spermidine and (d) nicotine are shown to demonstrate the divergent relationships in irTOC1 plants (blue bars) as compared to EV (black bars) or irZTL plants (yellow bars; $n = 6$ per genotype and timepoint, mean ± SE for all). While irZTL shows reductions in all compounds compared to EV, irTOC1 produces relatively more nicotine and less of the two phenolamides, leading to significant changes in the (e, f) trait correlations among these compounds for irTOC1 plants. Data in boxes refer to results of ANOVA tests; differing letters and asterisks represent significant differences in estimated marginal means of linear trends, extracted through Tukey-adjusted pairwise contrasts between genotypes, *, $P < 0.05$; **, $P < 0.01$; ***, $P < 0.001$; ns, not significant. Shading represents 95% confidence level intervals along correlation axes for (e) and (f). CoA, Coenzyme A.

between irZTL and irTOC1, while nicotine levels were 60% higher in irTOC1 relative to irZTL plants. Under control conditions, DCS levels were 72% lower in irTOC1 and 50% lower in irZTL relative to EV plants, while neither irZTL nor irTOC1 levels 72 hai were significantly different from EV levels (Fig. 2c).

Allocation of N is shifted towards nicotine in *TOC1*-silenced plants

Nicotine, CP, and DCS are N-rich compounds which are found in high abundance both constitutively and after herbivore induction and share an N-rich precursor, putrescine (Fig. 2a). We examined the allocation pattern of N among these three compounds using a ^{15}N-pulse labeling approach described previously in *N. attenuata* (Ullmann-Zeunert *et al.*, 2012, 2013), with both control and *M. sexta* W + OS-elicited plants being sampled at various time intervals over the next 4 d (Fig. 3a). To minimize the influence of phenology, irTOC1 plants were germinated 1 wk before EV plants, as they display 1-wk-delayed flowering (Yon *et al.*, 2012; Valim *et al.*, 2019). Final measured nicotine concentrations were 40% higher in irTOC1 relative to EV elicited leaves, while nicotine concentrations under control conditions

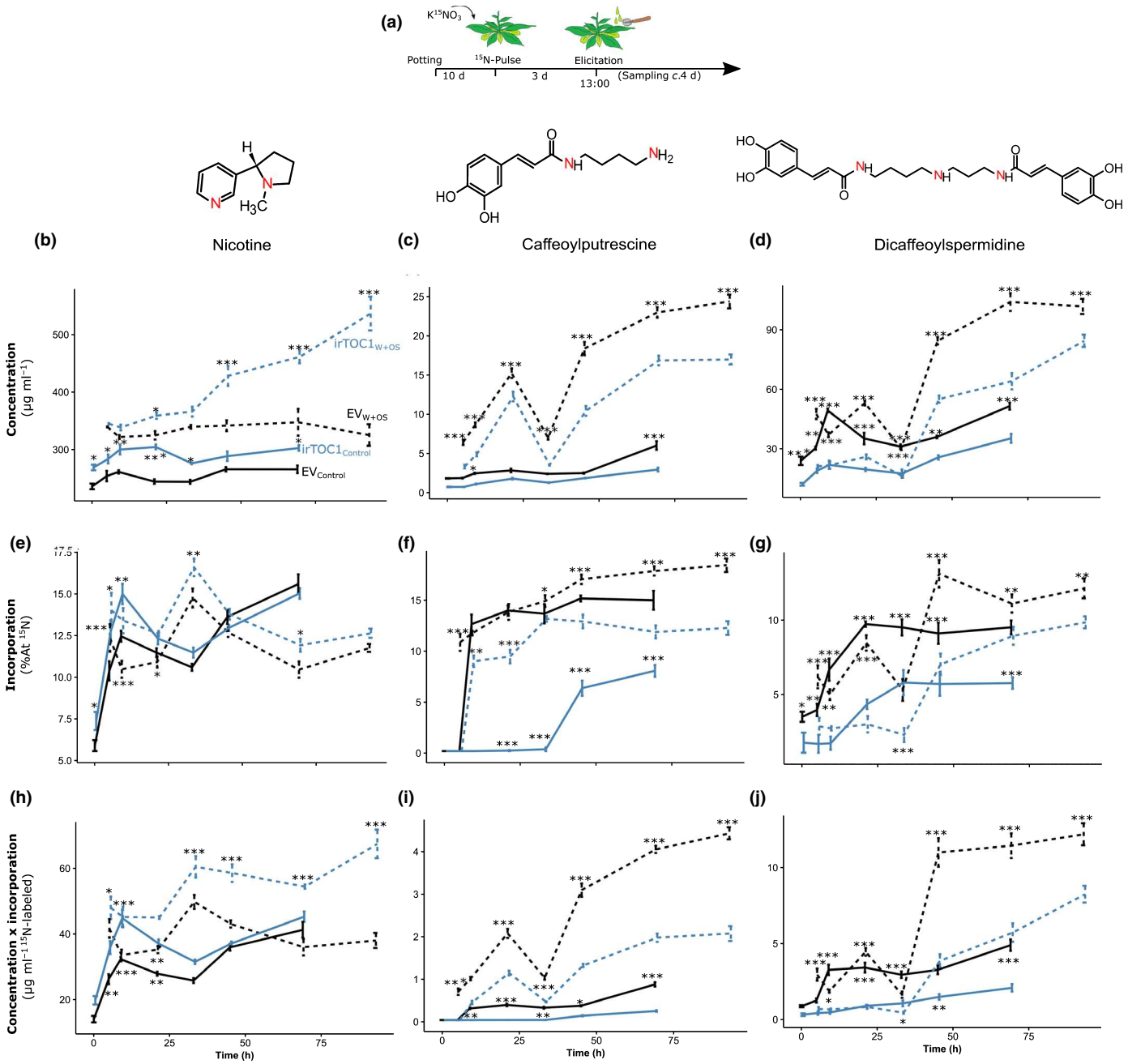

Fig. 3 Silencing *TOC1* in *Nicotiana attenuata* causes a shift in nicotine and phenolamide concentration and ^{15}N incorporation patterns. (a) Experimental design of ^{15}N-labeling experiments: plants were irrigated with ^{15}N-labeled KNO_3 3 d before the start of the experiment, at which plants were treated by controlled wounding and *Manduca sexta* oral secretions (W + OS) and sampled for 93 h to determine shifts in ^{15}N allocation between nicotine and the phenolamides caffeoylputrescine (CP) and dicaffeoyl spermidine (DCS). (b–d) Nicotine concentrations were increased in irTOC1 plants, while CP and DCS concentrations were decreased in irTOC1 plants relative to EV plants; these differences were further exacerbated by simulated herbivory elicitation. Similarly, (e–g) ^{15}N % atomic incorporation (%At ^{15}N) into nicotine was increased in irTOC1 plants, while CP and DCS %At ^{15}N were decreased in irTOC1 plants relative to EV plants. (h-j) The concentration of ^{15}N-labeled nicotine (µg/ml ^{15}N-labeled) was correspondingly increased in irTOC1 plants, while CP and DCS ^{15}N-labeled concentrations were decreased in irTOC1 plants relative to EV plants; as for the concentrations of each compound showin in (b-d), these differences were further exacerbated bysimulated herbivory elicitation. For (b-j), $n = 5$ per genotype, treatment, and timepoint, and means ± SEM are shown. Asterisks represent significant differences in estimated marginal means of linear trends, extracted through Tukey-adjusted pairwise contrasts, within one timepoint: *, $P < 0.05$; **, $P < 0.01$; ***, $P < 0.001$.

were largely unchanged (Fig. 3b). CP and DCS concentrations followed an inverse trend: CP concentrations were similar under control conditions between EV and irTOC1, while final measured CP concentrations were 30% higher in EV elicited plants (Fig. 3c); final measured DCS concentrations were 40% higher in EV control plants, and 25% higher in EV elicited plants (Fig. 3d).

Incorporation of ^{15}N (measured as % of atomic incorporation of ^{15}N, hereafter %At ^{15}N) was temporally shifted in irTOC1 and EV plants by the W + OS treatment for nicotine (Fig. 3e).

Final measured %At ^{15}N for CP was 50% lower in irTOC1 control plants, and 30% lower in irTOC1 elicited plants relative to EV (Fig. 3f). Final measured %At ^{15}N for DCS was 30% lower in irTOC1 control plants and 15% lower in irTOC1 elicited plants relative to EV (Fig. 3g).

Given the large differences in nicotine and phenolamide pools between EV and irTOC1 plants, mirroring differences in their concentrations (Fig. S1), we calculated the investment of ^{15}N into these metabolites by comparing the fractions of the nicotine and phenolamide pools synthesized from ^{15}N. These results showed that a larger fraction of ^{15}N-labeled nicotine accumulated in irTOC1 elicited plants (Fig. 3h), while larger fractions of ^{15}N-labeled CP accumulated in EV elicited plants (Fig. 3i). The fraction of ^{15}N-labeled DCS was larger in EV relative to irTOC1 elicited and control plants, although elicitation increased fractions in both genotypes (Fig. 3j). In summary, the patterns of ^{15}N incorporation as a fraction of metabolite concentration follow the same pattern as metabolite concentrations; however, irTOC1 plants preferentially invest ^{15}N into nicotine over phenolamides to a greater extent than predicted solely by the differences in concentration of these metabolites.

To explore allocation differences between nicotine and phenolamides in irTOC1 plants, we compared the normalized differences between nicotine and CP or DCS (e.g. nicotine − CP/nicotine + CP), for concentration and ^{15}N incorporation rates. This produced a normalized score where a value of +1 corresponds to only nicotine being detected; a value of −1 corresponds to only phenolamide being detected; and a value of 0 corresponds to equal abundances or incorporation rates being measured (Fig. 4b). Given the larger contribution of nicotine than phenolamide to the plant's biomass, normalized concentration differences for both EV and irTOC1 are heavily biased towards nicotine, with values between +1.00 and +0.85 for all time points, genotypes, and treatments for nicotine vs CP (Fig. 4c), and between +1.00 and +0.50 for nicotine vs DCS (Fig. 4d). Against this nicotine-biased background, elicitation shifted the proportion of nicotine and phenolamide pools towards CP or DCS, and both control and elicited EV plants were significantly shifted towards CP or DCS relative to irTOC1. The bias toward nicotine was less marked in normalized ^{15}N incorporation, with plants shifting towards greater incorporation into CP for elicited EV plants, and approaching 0 for elicited irTOC1 and control EV plants; however, control irTOC1 plants remained strongly nicotine-biased, with values above +0.5 until 45 hai (Fig. 4e). Patterns were similar for nicotine vs DCS ^{15}N incorporation, with control and elicited EV as well as elicited irTOC1 plants approaching 0, while elicited irTOC1 plants remained above +0.4 (Fig. 4f).

Blocking ethylene signaling by 1-methylcyclopropene treatment abolishes differences in nicotine accumulation between EV and *TOC1*-silenced plants

The JA-induced increase in nicotine accumulation in *N. attenuata* is suppressed by oral secretions of *M. sexta* larvae (Winz & Baldwin, 2001; Von Dahl *et al.*, 2007), and the observed increase in nicotine accumulation in irTOC1 plants after simulated herbivory mirrors the release from suppression in ethylene-deficient plants. However, the herbivory-elicited ethylene burst is not affected in *TOC1*-silenced plants (Fig. S2), and the transcript abundances of various components of the ethylene signaling pathway are not significantly affected by *TOC1* silencing (Fig. S3). To determine whether increased levels of nicotine in irTOC1 plants were related to ethylene perception, rosette stage plants (10 d after potting) were treated with 1-methylcyclopropene (1-MCP) inside of a Plexiglas chamber for 8 h overnight and re-acclimated to glasshouse conditions for 7 h before elicitation at 13:00 h (Fig. 5a). As for the ^{15}N-labeling experiment, irTOC1 plants were germinated 1 wk early. 1-MCP is an ethylene agonist that binds to the ethylene receptor ETR1 and prevents inactivation of downstream ethylene-sensitive transcription factors (Fig. 5b; see Wang *et al.*, 2002; Blankenship & Dole, 2003; Watkins, 2006; Ju & Chang, 2015). Differences in nicotine accumulation after W + OS elicitation between EV and irTOC1 plants were abolished by 1-MCP treatment (Fig. 5c), while accumulation of CP increased proportionally after 1-MCP treatment, remaining lower in irTOC1 plants (Fig. 5e). DCS levels were slightly increased in EV plants after 1-MCP treatment and elicitation, and remained significantly higher than irTOC1 plants (Fig. 5g). We analyzed root metabolite levels and also observed a decrease in the variation of nicotine levels between roots of EV and irTOC1 plants treated with 1-MCP (Fig. 5d). Consistent with previous findings, CP and DCS were not consistently detected in roots, and the low levels which were detected did not change significantly as a result of treatment (Fig. 5f,h).

To further test *TOC1*'s role in regulating ethylene sensitivity, we performed an ethylene triple response assay, a classic tool for exploring ethylene responses (Merchante & Stepanova, 2017). We compared the responses of irTOC1, EV, and 35S-etr1 seedlings germinating in a gradient of 1-aminocyclopropane-1-carboxylic acid (ACC), an ethylene precursor, under dark conditions. 35S-etr1 seedlings express the Arabidopsis etr1-1 mutant receptor, rendering plants unresponsive to ethylene (von Dahl *et al.*, 2007). In EV or wild-type seedlings, exposure to even minute concentrations of ACC (0.2 μM) is sufficient to observe the expected response, consisting of a shortening and thickening of the hypocotyl as well as an exaggeration of apical hook curvature in Arabidopsis. In *N. attenuata*, although the effect of ethylene on the thickness of the hypocotyl was less obvious, hypocotyl shortening provided a reliable metric for quantifying ethylene sensitivity (Fig. S4a) of EV, which is highly sensitive and displays hypocotyl shortening at concentrations of 0.2 μM. Two independent irTOC1 lines were not responsive to 0.2 μM ACC, and displayed more elongated hypocotyls under 0.5 μM ACC concentrations compared to EV; as expected, 35S-etr1 was unresponsive to any tested concentration of ACC (Fig. S4b).

TOC1 in roots limits nicotine accumulation, but changes to reproductive allocation depend on *TOC1* in shoots

Given that nicotine is synthesized in the roots, and that changes in the allocation of N among metabolically expensive compounds

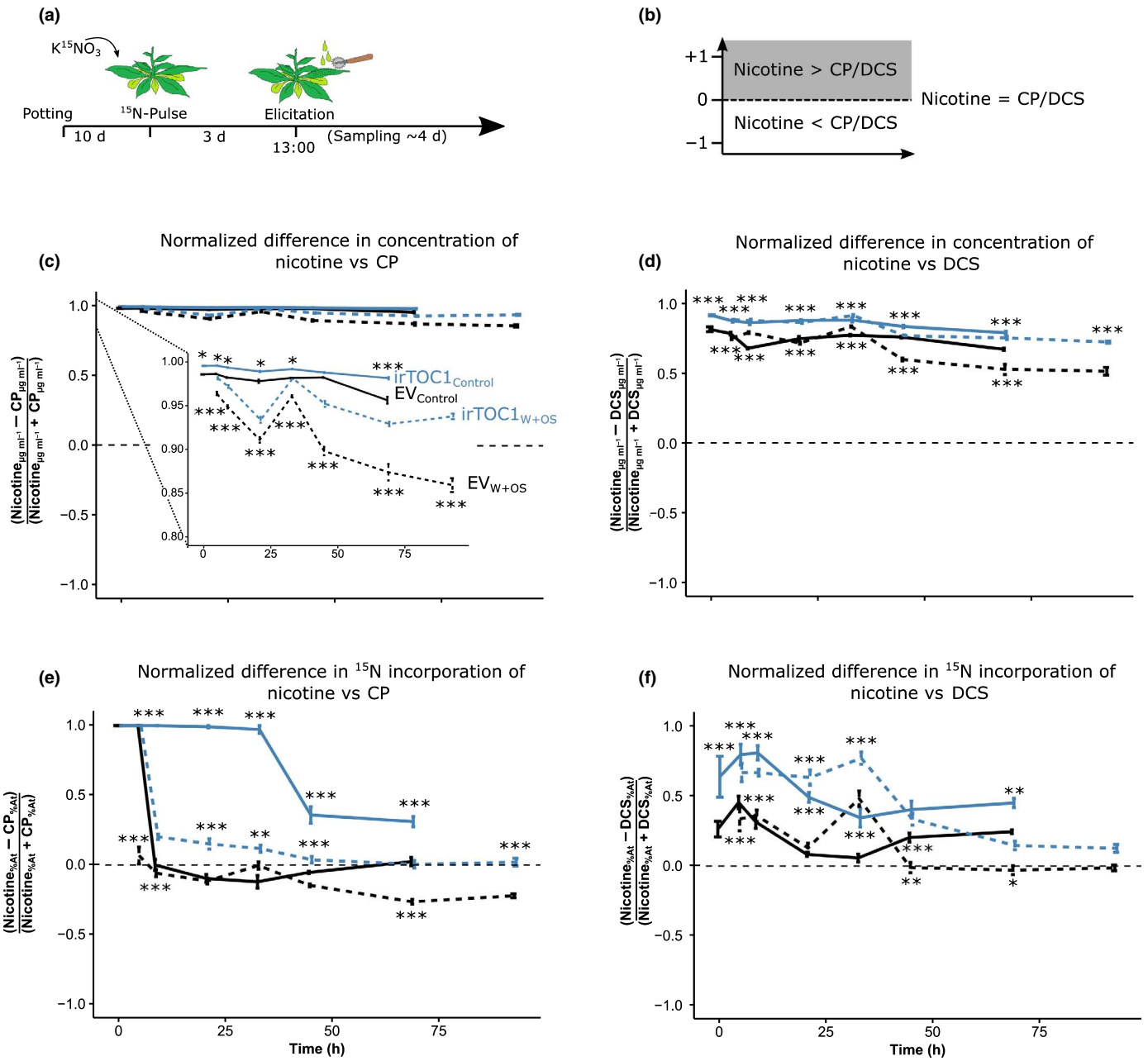

Fig. 4 Silencing *TOC1* in *Nicotiana attenuata* causes a shift in N allocation patterns away from phenolamides and towards nicotine. (a) Experimental design of ^{15}N-labeling experiments: plants were irrigated with ^{15}N-labeled KNO_3 3 d before the start of the experiment, at which plants were treated by controlled wounding and *Manduca sexta* oral secretions (W + OS) and sampled for 93 h to determine shifts in ^{15}N allocation between nicotine and the phenolamides caffeoylputrescine (CP) and dicaffeoyl spermidine (DCS). (b) Concentrations and ^{15}N incorporation rates were normalized between nicotine and the two phenolamides CP and DCS, using the equation (nicotine − phenolamide)/(nicotine + phenolamide). These produced normalized differences that can be interpreted as exemplified in the following figure, such that a value of > 0 denotes greater values for nicotine, a value = 0 denotes equal values for nicotine and the phenolamide, and a value of < 0 denotes greater values for the phenolamide. (c, d) CP and DCS normalized concentration differences showed marked biases towards nicotine, although significant differences between EV and irTOC1 plants were observed ($n = 5$ per genotype, treatment and time point; means ± SEM are shown). (e, f) Normalized ^{15}N incorporation differences showed more equivalence between nicotine and CP/DCS, with significant differences between EV and irTOC1 plants also observed ($n = 5$ per genotype, treatment and time point; means ± SEM are shown). Asterisks represent significant differences in estimated marginal means of linear trends, extracted through Tukey-adjusted pairwise contrasts, within one timepoint: *, $P < 0.05$; **, $P < 0.01$; ***, $P < 0.001$.

might affect the plant's ability to defend itself against herbivores, we examined the effect of tissue-specific silencing of *TOC1* by using a micrografting approach under field conditions to generate a heterograft silenced in *TOC1* in roots only (EV/irTOC1, hereafter ET heterografts) or in whole plants (irTOC1/irTOC1, hereafter TT homografts) as well as control grafts with EV roots and shoots (EV/EV, hereafter EE homografts; Fig. 6a). The increased nicotine accumulation of the heterograft (EE – ET:

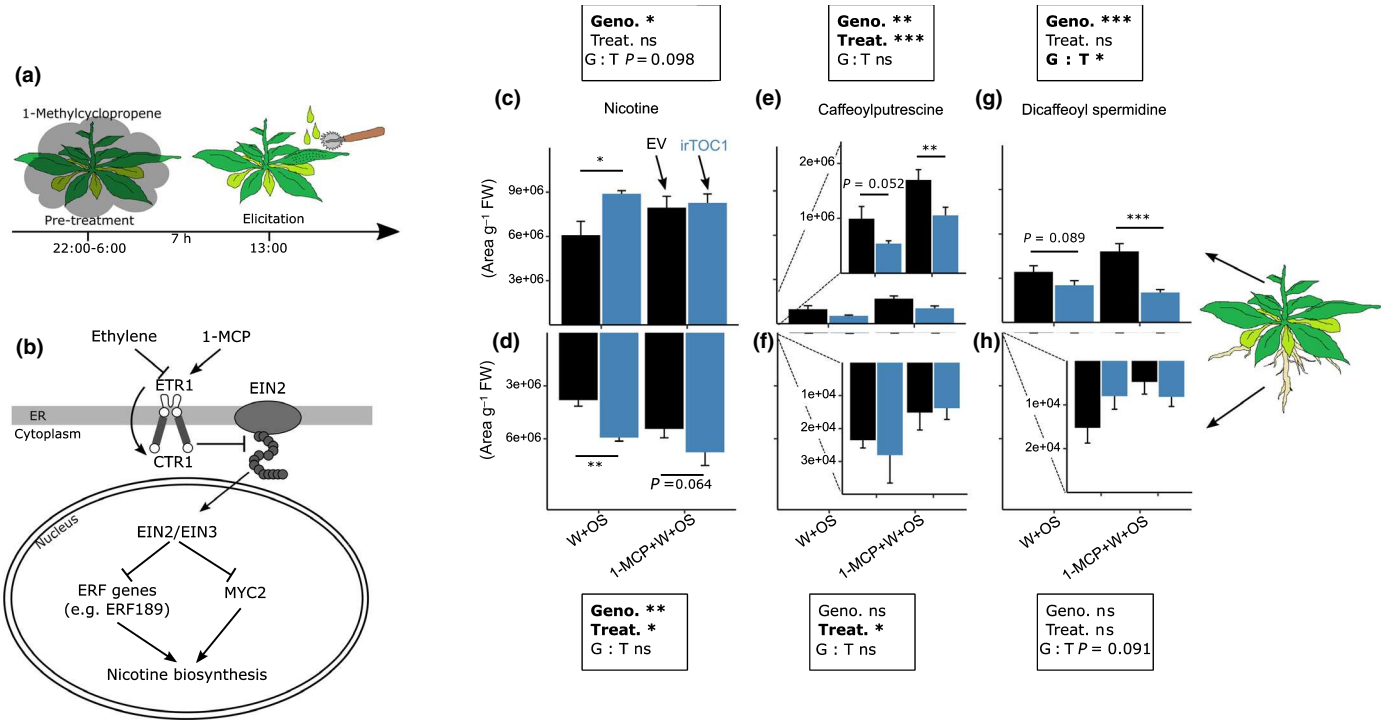

Fig. 5 Shifts in nicotine levels after wounding and 1-methylcyclopropene treatment are consistent with an abrogated ethylene signaling/feedback loop in irTOC1 plants. (a) Treatment and sampling scheme for the 1-methylcyclopropene (1-MCP) experiment. (b) 1-MCP acts as an ethylene agonist, preventing ethylene from engaging in downstream signaling that modulates biosynthesis of nicotine in *Nicotiana attenuata*. Nicotine accumulation in (c) leaves and (d) roots of EV (black) and irTOC1 (blue) plants is presented for plants treated with and without 1-MCP, in addition to *Manduca sexta* wounding and oral secretions (W + OS and 1-MCP + W + OS, respectively). Accumulations of the inducible phenolamide caffeoylputrescine in (e) leaves and (f) roots and the constitutive phenolamide dicaffeoyl spermidine in the (g) leaves and (h) roots are presented on the same scale; insets provide visualization of significant differences at low abundances (e, f, h; $n = 4$–5 per genotype and treatment, mean + SE for all panels). Data in boxes refer to results of ANOVA tests; asterisks represent the significance of irTOC1 values to those of EV extracted using Tukey-adjusted pairwise contrasts, within one timepoint: *, $P < 0.05$; **, $P < 0.01$; ***, $P < 0.00$; ns, not significant.

$P < 0.04$) mirrored the levels of nicotine in TT homografts (Fig. 6b; EE – TT: $P < 0.04$, pairwise *t*-tests across treatments, Holm-Bonferroni *P*-value adjustment). The reduction in W + OS-elicited CP levels observed in TT homografts was abolished in ET heterografts, and levels between treatments were significantly different across genotypes (Fig. 5c; Control – Elicited: $P = 0.029$, pairwise *t*-tests across treatments, Holm-Bonferroni *P*-value adjustment). Curiously, DCS levels showed an increase in ET heterografts, but not in TT homografts relative to EE homografts (Fig. 6d; EE – ET: $P = 0.028$, EE – TT: $P = 0.087$, pairwise *t*-tests across treatments, Holm-Bonferroni *P*-value adjustment). A similar pattern was observed for the accumulation of the N-free polyphenol chlorogenic acid, with levels being attenuated in irTOC1 plants and TT homografts (Fig. S5b).

ET plants did not exhibit fitness reductions associated with increased nicotine accumulation, rather having a 33% increase in seed capsule production 40 d after planting (dap) compared to EE control plants (Fig. 6e, EE – ET: $P = 0.0005$, Tukey contrasts by genotype). Unlike TT plants, both ET and EE elicited plants experienced a 50–60% decrease in seed capsule production by 40 dap (Fig. 6e, $EE_{Control} - EE_{W+OS}$: $P < 0.0001$; $EE_{Control} - EE_{W+OS}$: $P = 0.0051$; Tukey contrasts by treatment). Flower production was similarly affected by elicitation in EE and ET plants (Fig. 6f). By contrast, TT aboveground and belowground biomass were decreased 45–50% by elicitation, with TT control roots being more massive than EE control shoots (Fig. 6g, $EE_{Control - TTControl}$: $P = 0.0114$, $ET_{Control} - TT_{Control}$: $P = 0.0708$) and with TT control roots more massive than EE and ET control roots (Fig. 6h, $EE_{Control} - TT_{Control}$: $P = 0.0067$, $ET_{Control} - TT_{Control}$: $P = 0.0358$; Tukey contrasts by treatment). Elicited plants had similar above- and belowground biomass.

Discussion

Selective allocation by plants, both of resources to defense vs growth and reproduction, and of defense traits among tissues, is a common theme in theories of plant defense (McKey, 1974; Herms & Mattson, 1992; Meldau *et al.*, 2012). Although plant defense theories generally do not consider the temporal dimension of selective allocation, two frameworks, apparency theory and optimal defense theory, incorporate different probabilities of herbivore attack based on plant phenotypes. In particular, optimal defense theory predicts that tissue defense should be correlated with the likelihood of attack and tissue value (Zangerl & Rutledge, 1996; Meldau & Baldwin, 2013). This could also be considered in terms of diurnal changes in likelihood of attack, in addition to the traditional view of changing likelihood over ontogeny. Previous work in *N. attenuata* is consistent with the

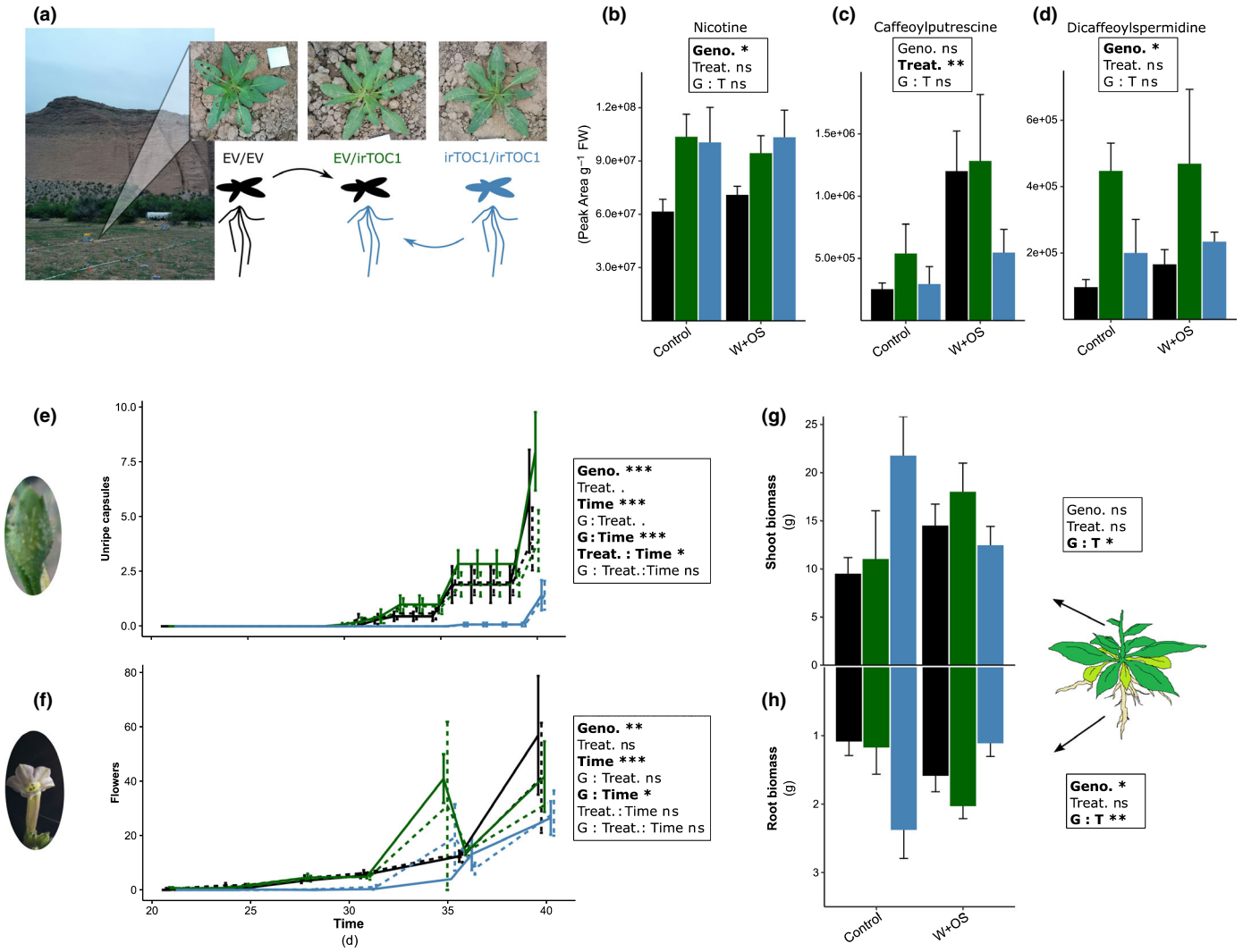

Fig. 6 Silencing *TOC1* in the shoot causes a severe fitness reduction under field conditions, while root *TOC1* silencing is sufficient to explain differential nicotine accumulation compared to EV. (a) Representation of field plot at Lytle Preserve, UT, USA, as well as representative photos of EV/EV (black), EV/irTOC1 (green), and irTOC1/irTOC1 (blue) micrografted plants at the time of treatment and sampling. (b–d) Production of secondary metabolites: nicotine (b), caffeoylputrescine (c), and dicaffeoylspermidine (d) at 72 h after elicitation with wounding and application of *Manduca sexta* oral secretions (W + OS; $n = 4$–6, mean + SE). (e) Unripe seed capsules and (f) flowers during the extent of the field season across all genotypes and treatments ($n = 11$–13, mean ± SE). (g) Shoot and (h) root biomass at the end of the field season, 54 d after planting ($n = 4$–6, mean + SE). Data in boxes refer to results of ANOVA tests; asterisks represent significant differences ($P < 0.05$) in estimated marginal means of linear trends, extracted through Tukey-adjusted pairwise contrasts: *, $P < 0.05$; **, $P < 0.01$; ***, $P < 0.00$; ns, not significant.

predictions of optimal defense theory: inducible defenses in *N. attenuata* are regulated by levels of cytokinins, a class of developmental growth hormones (Brütting *et al.*, 2017), and developmental transitions such as flowering alter the ethylene/JA-mediated defense signaling at the heart of inducible plant defenses (Diezel *et al.*, 2011). However, the role of the circadian clock in optimizing defenses across development has not been previously investigated.

Our results provide new mechanistic insight into the circadian clock's role in optimizing the allocation of resources in *N. attenuata*'s defense chemistry, building on the evidence outlined in Li *et al.* (2018) that the clock component ZTL interacts with jasmonate signaling to promote synthesis of the abundant, N-rich defense compound nicotine. Here, we find that *TOC1* interacts with ethylene signaling to dampen nicotine accumulation, and that *TOC1* additionally mediates the allocation of N between nicotine and another group of abundant N-containing defense compounds, the phenolamides. The increase in elicited nicotine levels in particular fit the current model of TOC1-ZTL interaction, given that TOC1 indirectly inhibits ZTL by repressing GI (Fig. 1a; Makino *et al.* 2001), and ZTL in turn targets TOC1 for degradation (Fujiwara *et al.* 2008).

Testing the functional consequences of these allocation differences under field conditions demonstrates that these trade-offs in N allocation do not explain the large effect of TOC1 function on plant fitness, which furthermore seems to be specific to the function of TOC1 in shoots, while nicotine is synthesized in the root and then transported to the shoot. Furthermore, correcting for

phenological differences between irTOC1 and EV plants did not affect these patterns of defense compound accumulation, indicating a potentially tissue-specific function of *TOC1* in defense metabolite production. Given that the circadian clock has been shown to be mechanistically distinct (Endo *et al.*, 2014) and to vary in functional outputs across tissue types (Bordage *et al.*, 2016), there should be a greater effort to explore the functional consequences of individual circadian clock components across tissues for defense responses.

Another theory of plant defense that has been applied in understanding resource allocation, the carbon/nutrient balance theory, predicts that resources such as carbon or macronutrients such as N, phosphorus, or potassium may be rate-limiting for growth or defense compound production (Bryant *et al.*, 1983; Massad *et al.*, 2012). Nitrogen pools in particular provide a valuable testing ground for questions of resource allocation. They can be highly limited and are subject to changing needs and intense intraspecific competition in *N. attenuata* populations, and many of *N. attenuata*'s highly abundant defense metabolites, including nicotine and phenolamides, are N-rich (Baldwin *et al.*, 1998; van Dam & Baldwin, 2001; Ullmann-Zeunert *et al.*, 2013). Resource allocation can be manipulated directly by the circadian clock, as has been shown for carbon metabolism (Sanchez-Villarreal *et al.*, 2013; Müller *et al.*, 2014; Kölling *et al.*, 2015). Our results suggest that TOC1 modulates N allocation indirectly as an output of defense signaling (Figs 3, 4), given that levels of chlorogenic acid (CGA) are also attenuated in irTOC1 plants, and CGA is a polyphenolic compound also regulated by *MYB8* much like CP and DCS (Fig. S5). The different effects of ZTL and TOC1 on the accumulation of N-rich defense metabolites (Fig. 2) as well as TOC1's apparent role in ethylene-mediated defense signaling (Fig. 5) indicate that individual members of the circadian clock have specific roles in regulating plant responses to herbivory.

Previous data suggest that herbivory disrupts normal clock function and its outputs (Joo *et al.*, 2018). It may be that, whatever the adaptive value of circadian-regulated inducibility of JA or defense metabolite production, plant resources are preferentially if temporarily mobilized for defense after elicitation occurs. Our results are consistent with this expectation. We find that that simulated herbivory elicitation shifts %At ^{15}N towards phenolamides and away from nicotine in both EV and irTOC1 plants, although differences remain significant between the two genotypes: only EV plants incorporate greater amounts of ^{15}N into CP rather than nicotine (Fig. 4e). This highlights an important difference between investigating variation in accumulation vs allocation. The effect of TOC1 is harder to observe when comparing concentrations and total secondary metabolite accumulation after elicitation (Figs 2, 3b–d, S1b–d).

Although circadian clock outputs are not always rhythmic, rhythmic phenotypes may point towards novel functions for clock components. Ethylene emissions are rhythmic and ethylene signaling is regulated by the circadian clock in Arabidopsis (Thain *et al.*, 2004; Song *et al.*, 2018). Previous work has shown that ethylene-insensitive mutants overproduce ethylene but do not display altered rhythmicity in ethylene production (Thain *et al.*, 2004). Despite this, our results provide evidence that for a well-known ethylene response – the dampening of herbivore-elicited nicotine accumulation – the circadian clock component *TOC1* seems to play a key role in signal transduction. The induction of ethylene after elicitation with *M. sexta* oral secretions is not diminished by *TOC1* silencing, but rather tends to increase, consistent with the hypothesis that *TOC1* abrogation may lead to impaired ethylene sensitivity (Figs 5, S2). This is supported by a triple response assay demonstrating reduced ethylene sensitivity of irTOC1 plants (Fig. S4).

The ecological significance of ethylene-mediated nicotine dampening under field conditions remains unclear, given that nicotine levels remained high even without experimental elicitation in the field (Fig. 6b). This could be due to the presence of generalist herbivores, which may elicit plants under natural conditions independently of experimental manipulations (even when herbivore exclusion is attempted e.g. with insecticide; see McGale *et al.*, 2018). Ethylene signaling prevents a surge of nicotine in plants elicited by the nicotine-tolerant *M. sexta* (von Dahl *et al.*, 2007), but is likely not relevant for plants already using nicotine to defend against nicotine-susceptible generalists. It is thus possible that further field studies would yield different degrees of nicotine production in response to experimental elicitation, with the elicited peak in irTOC1 plants more obvious under conditions with fewer generalist herbivores. We note that the more *M. sexta*-specific induction of CP was observed (Fig. 6c). Thus, our field experiments demonstrate that even under less controlled and more realistic conditions, the shifted ratio between nicotine and phenolamides in *TOC1*-silenced plants persists (Fig. 6). Micrografting of *TOC1*-silenced roots to EV shoots demonstrates that TOC1's role in regulating herbivore-elicited phenolamide production is likely shoot-specific, while TOC1's role in control of nicotine biosynthesis is root-specific.

TOC1 is known to be involved in flowering time regulation, and this is observed under field conditions for whole-plant *TOC1* silencing (Valim *et al.*, 2019). In *N. attenuata*, the onset of flowering attenuates the elicitation of defense compounds (Diezel *et al.*, 2011), and whole-plant *TOC1*-silencing may thus change the responsiveness of plants to elicitation over their lifetime. However, developmental timing did not explain the shift in defenses between nicotine and phenolamides observed in irTOC1 plants, as both plants that were developmentally matched by offsetting germination (Figs 3–5), as well as plants that were germinated synchronously (Figs 1, 2, 6), exhibited the same shifts in nicotine and phenolamide production. Furthermore, using a micrografting approach under field conditions, root *TOC1*-silenced heterografts with wild-type phenology produced greater amounts of nicotine (Fig. 6b), despite no apparent fitness consequences (Fig. 6e,f). As discussed in the previous paragraph, nicotine did not respond to induction in the field, unlike CP, indicating that all grafted genotypes remained sensitive to induction (and that nicotine was already responding to ambient herbivory). Together, our data suggest that phenological functions of *TOC1* affect plant fitness, but do not explain differential production of N-rich defense compounds.

Given that the fitness metrics of root-only *TOC1*-silenced heterografts remained similar to EV plants under field

conditions, the fitness consequences of whole-plant *TOC1* silencing may have less to do with a differential allocation of N generally, and more to do with a specific shift towards overproduction of a single defense metabolite such as nicotine at the expense of a more diverse defensive metabolite profile. It should be noted that our field data cannot fully disentangle phenological from metabolic effects on plant fitness, as ET grafts differ from TT grafts in both phenology and phenolamide production. Future work should dissect to what extent the fitness disadvantages of irTOC1 and other clock-altered plants under field conditions are due to allocation costs, or to the opportunity costs of mistimed defenses. It should be noted that *TOC1* has drastic effects on plant drought responses, both in seedlings under laboratory conditions (Legnaioli *et al.*, 2009) as well as under field conditions (Valim *et al.*, 2019). However, there is little evidence under field conditions for an interactive effect between drought and herbivory; a recent study using 16 soybean genotypes failed to find any interactive effects of drought and herbivory on plant performance (Grinnan *et al.*, 2013). The results of the ^{15}N-labeling experiment (Figs 3, 4), together with previous work by Joo *et al.* (2018), suggest that the circadian machinery plays a greater role in the metabolic state of the plant preceding and immediately at the beginning of herbivory events, and that herbivory-elicited metabolic reorganization decouples the clock from its normal function under control conditions. The use of inducible promoters (see e.g. Schäfer *et al.*, 2013) may help to dissect the role of the clock in basal or preparatory stages before herbivory, as well as the role of circadian clock components such as TOC1 and ZTL in the mobilization of defense responses during herbivory.

One test of the herbivory disruption hypothesis would be to measure whether herbivores feeding at different times of the day perform differently on clock-shifted plants, with or without prior elicitation. Performance differences are observed for rhythmically feeding *Trichoplusia ni* on clock-disrupted vs wild-type Arabidopsis plants without pre-elicitation (Goodspeed *et al.*, 2012). The disruption hypothesis predicts that pre-elicitation would reduce this difference. Alternatively, clock components may function in the mobilization of defense apart from their timekeeping function, in which case knocking out or down these components (including TOC1 and ZTL) may affect plant susceptibility and herbivore performance regardless of either elicitation, or whether herbivores display rhythmic feeding. Performing such experiments under field conditions, while more realistic, makes them difficult to interpret given the many effects of the clock on phenology. Performing experiments at different times of the season should further elucidate the effect of phenology on the clock's role in plant defense, as it has done for yield (Izawa *et al.*, 2011). This could elucidate interactions of phenology with environmental cues in defense, similarly to the coincidence model of photoperiodic flowering, which requires both functioning circadian rhythms and appropriate seasonal stimuli.

Acknowledgements

We thank the glasshouse department at the Max Planck Institute for Chemical Ecology and the field team in 2015 and 2016 for support; Brigham Young University for the use of the Lytle Ranch Preserve field station in Utah, USA, and APHIS for constructive regulatory oversight; the technical staff at the department of Molecular Ecology for providing seeds; L. Cortes-Llorca for helpful discussions; K. Groten for suggesting a triple response assay to test ethylene sensitivity; and both the International Max Planck Research School (IMPRS) on the Exploration of Ecological Interactions with Chemical and Molecular Techniques and the Young Biodiversity Research Training Group (yDiv) for their support of HV and EM.

Author contributions

Conceptualization and project administration: ITB, MCS, EG; methodology and investigation: HV, HD, YJ, EM, ITB, MCS, EG, RH; formal analysis: HV, HD, YJ; writing – original draft: HV; writing – review and editing: HD, YJ, EM, RH, EG, ITB, MCS; resources: ITB, MCS; visualization: HV, HD, EG, MCS; supervision, ITB, EG and MCS; funding acquisition: ITB.

ORCID

Ian T. Baldwin https://orcid.org/0000-0001-5371-2974
Emmanuel Gaquerel https://orcid.org/0000-0003-0796-6417
Rayko Halitschke https://orcid.org/0000-0002-1109-8782
Youngsung Joo https://orcid.org/0000-0001-8245-7693
Erica McGale https://orcid.org/0000-0002-5996-4213
Meredith C. Schuman https://orcid.org/0000-0003-3159-3534
Henrique Valim https://orcid.org/0000-0001-9447-4773

References

Arimura G, Köpke S, Kunert M, Volpe V, David A, Brand P, Dabrowska P, Maffei ME, Boland W. 2008. Effects of feeding *Spodoptera littoralis* on lima bean leaves: IV. Diurnal and nocturnal damage differentially initiate plant volatile emission. *Plant Physiology* **146**: 965–973.

Baldwin IT, Gorham D, Schmelz EA, Lewandowski CA, Lynds GY. 1998. Allocation of nitrogen to an inducible defense and seed production in *Nicotiana attenuata*. *Oecologia* **115**: 541–552.

Baldwin IT, Ohnmeiss TE. 1994. Swords into plowshares? *Nicotiana sylvestris* does not use nicotine as a nitrogen source under nitrogen-limited growth. *Oecologia* **98**: 385–392.

Baldwin IT, Staszak-Kozinski L, Davidson R. 1994. Up in smoke: I. Smoke-derived germination cues for postfire annual, *Nicotiana attenuata* torr. Ex. Watson. *Journal of Chemical Ecology* **20**: 2345–2371.

Baldwin IT, Zhang ZP, Diab N, Ohnmeiss TE, McCloud ES, Lynds GY, Schmelz EA. 1997. Quantification, correlations and manipulations of wound-induced changes in jasmonic acid and nicotine in *Nicotiana sylvestris*. *Planta* **201**: 397–404.

Blankenship SM, Dole JM. 2003. 1-Methylcyclopropene: a review. *Postharvest Biology and Technology* **28**: 1–25.

Bordage S, Sullivan S, Laird J, Millar AJ, Nimmo HG. 2016. Organ specificity in the plant circadian system is explained by different light inputs to the shoot and root clocks. *New Phytologist* **212**: 136–149.

Brütting C, Schäfer M, Vanková R, Gase K, Baldwin IT, Meldau S. 2017. Changes in cytokinins are sufficient to alter developmental patterns of defense metabolites in *Nicotiana attenuata*. *The Plant Journal* **89**: 15–30.

Bryant JP, Chapin FS III, Klein DR. 1983. Carbon/nutrient balance of boreal plants in relation to vertebrate herbivory. *Oikos* **40**: 357–368.

Bubner B, Gase K, Berger B, Link D, Baldwin IT. 2006. Occurrence of tetraploidy in *Nicotiana attenuata* plants after *Agrobacterium*-mediated transformation is genotype specific but independent of polysomaty of explant tissue. *Plant Cell Reports* **25**: 668–675.

Chapin FS III, Schulze E-D, Mooney HA. 1990. The ecology and economics of storage in plants. *Annual Review of Ecology and Systematics* **21**: 423–447.

Chini A, Fonseca S, Fernández G, Adie B, Chico JM, Lorenzo O, García-Casado G, López-Vidriero I, Lozano FM, Ponce MR *et al.* 2007. The JAZ family of repressors is the missing link in jasmonate signalling. *Nature* **448**: 666–671.

Cook RD, Weisberg S. 1982. *Residuals and influence in regression.* New York, NY, USA: Chapman & Hall.

van Dam NM, Baldwin IT. 2001. Competition mediates costs of jasmonate-induced defences, nitrogen acquisition and transgenerational plasticity in *Nicotiana attenuata*. *Functional Ecology* **15**: 406–415.

Diezel C, Allmann S, Baldwin IT. 2011. Mechanisms of optimal defense patterns in *Nicotiana attenuata*: flowering attenuates herbivory-elicited ethylene and jasmonate signaling. *Journal of Integrative Plant Biology* **53**: 971–983.

Endo M, Shimizu H, Nohales MA, Araki T, Kay SA. 2014. Tissue-specific clocks in *Arabidopsis* show asymmetric coupling. *Nature* **515**: 419–422.

Fragoso V, Goddard H, Baldwin IT, Kim SG. 2011. A simple and efficient micrografting method for stably transformed *Nicotiana attenuata* plants to examine shoot-root signaling. *Plant Methods* **7**: 1–8.

Fujiwara S, Wang L, Han L, Suh S-S, Salomé PA, McClung CR, Somers DE. 2008. Post-translational regulation of the Arabidopsis circadian clock through selective proteolysis and phosphorylation of pseudo-response regulator proteins. *Journal of Biological Chemistry* **283**: 23073–23083.

Gaquerel E, Gulati J, Baldwin IT. 2014. Revealing insect herbivory-induced phenolamide metabolism: from single genes to metabolic network plasticity analysis. *The Plant Journal* **79**: 679–692.

Gaquerel E, Heiling S, Schoettner M, Zurek G, Baldwin IT. 2010. Development and validation of a liquid chromatography-electrospray ionization-time-of-flight mass spectrometry method for induced changes in *Nicotiana attenuata* leaves during simulated herbivory. *Journal of Agricultural and Food Chemistry* **58**: 9418–9427.

Goodspeed D, Chehab EW, Covington MF, Braam J. 2013a. Circadian control of jasmonates and salicylates: the clock role in plant defense. *Plant Signaling & Behavior* **8**: 20–23.

Goodspeed D, Chehab EW, Min-Venditti A, Braam J, Covington MF. 2012. *Arabidopsis* synchronizes jasmonate-mediated defense with insect circadian behavior. *Proceedings of the National Academy of Sciences, USA* **109**: 4674–4677.

Goodspeed D, Liu JD, Chehab EW, Sheng Z, Francisco M, Kliebenstein DJ, Braam J. 2013b. Postharvest circadian entrainment enhances crop pest resistance and phytochemical cycling. *Current Biology* **23**: 1235–1241.

Greenham K, McClung CR. 2015. Integrating circadian dynamics with physiological processes in plants. *Nature Reviews Genetics* **16**: 598–610.

Grinnan R, Carter TE, Johnson MTJ. 2013. The effects of drought and herbivory on plant-herbivore interactions across 16 soybean genotypes in a field experiment. *Ecological Entomology* **38**: 290–302.

Gulati J, Baldwin IT, Gaquerel E. 2014. The roots of plant defenses: integrative multivariate analyses uncover dynamic behaviors of gene and metabolic networks of roots elicited by leaf herbivory. *The Plant Journal* **77**: 880–892.

Halitschke R, Keßler A, Kahl J, Lorenz A, Baldwin IT. 2000. Ecophysiological comparison of direct and indirect defenses in *Nicotiana attenuata*. *Oecologia* **124**: 408–417.

Halitschke R, Schittko U, Pohnert G, Boland W, Baldwin IT, Jena D. 2001. Molecular interactions between the specialist herbivore *Manduca sexta* (Lepidoptera, Sphingidae) and its natural host *Nicotiana attenuata*. III. Fatty acid-amino acid conjugates in herbivore oral secretions are necessary and sufficient for herbivore-specific plant responses. *Plant Physiology* **125**: 711–717.

Herden J, Meldau S, Kim SG, Kunert G, Joo Y, Baldwin IT, Schuman MC. 2016. Shifting *Nicotiana attenuata*'s diurnal rhythm does not alter its resistance to the specialist herbivore *Manduca sexta*. *Journal of Integrative Plant Biology* **58**: 656–668.

Herms DA, Mattson WJ. 1992. The dilemma of plants: to grow or defend. *Quarterly Review of Biology* **67**: 283–335.

Izawa T. 2012. Physiological significance of the plant circadian clock in natural field conditions. *Plant, Cell & Environment* **35**: 1729–1741.

Izawa T, Mihara M, Suzuki Y, Gupta M, Itoh H, Nagano AJ, Motoyama R, Sawada Y, Yano M, Hirai MY *et al.* 2011. *Os-GIGANTEA* confers robust diurnal rhythms on the global transcriptome of rice in the field. *Plant Cell* **23**: 1741–1755.

Joo Y, Fragoso V, Yon F., Baldwin IT, Kim S-G. 2017. Circadian clock component, LHY, tells a plant when to respond photosynthetically to light in nature. *Journal of Integrative Plant Biology* **59**: 572–587.

Joo Y, Schuman MC, Goldberg JK, Wissgott A, Kim S-G, Baldwin IT. 2018. Herbivory elicits changes in green leaf volatile production via jasmonate signaling and the circadian clock. *Plant, Cell & Environment* **42**: 972–982.

Ju C, Chang C. 2015. Mechanistic insights in ethylene perception and signal transduction. *Plant Physiology* **169**: 85–95.

Kahl J, Siemens DH, Aerts RJ, Gäbler R, Kühnemann F, Preston CA, Baldwin IT. 2000. Herbivore-induced ethylene suppresses a direct defense but not a putative indirect defense against an adapted herbivore. *Planta* **210**: 336–342.

Kang JH, Wang L, Giri A, Baldwin IT. 2006. Silencing *threonine deaminase* and *JAR4* in *Nicotiana attenuata* impairs jasmonic acid-isoleucine-mediated defenses against *Manduca sexta*. *Plant Cell* **18**: 3303–3320.

Karban R, Baldwin IT. 1997. Induced responses to herbivory. *Trends in Ecology & Evolution* **13**: 83.

Kaur H, Heinzel N, Schöttner M, Baldwin IT, Gális I. 2010. R2R3-NaMYB8 regulates the accumulation of phenylpropanoid-polyamine conjugates, which are essential for local and systemic defense against insect herbivores in *Nicotiana attenuata*. *Plant Physiology* **152**: 1731–1747.

Kim SG, Yon F, Gaquerel E, Gulati J, Baldwin IT. 2011. Tissue specific diurnal rhythms of metabolites and their regulation during herbivore attack in a native Tobacco, *Nicotiana attenuata*. *PLoS ONE* **6**: e26214.

Kölling K, Thalmann M, Müller A, Jenny C, Zeeman SC. 2015. Carbon partitioning in *Arabidopsis thaliana* is a dynamic process controlled by the plants metabolic status and its circadian clock. *Plant, Cell & Environment* **38**: 1965–1979.

Krügel T, Lim M, Gase K, Halitschke R, Baldwin IT. 2002. *Agrobacterium*-mediated transformation of *Nicotiana attenuata*, a model ecological expression system. *Chemoecology* **12**: 177–183.

Kumar P, Pandit SS, Steppuhn A, Baldwin IT. 2014. Natural history-driven, plant-mediated RNAi-based study reveals *CYP6B46*'s role in a nicotine-mediated antipredator herbivore defense. *Proceedings of the National Academy of Sciences, USA* **111**: 1245–1252.

Legnaioli T, Cuevas J, Mas P. 2009. *TOC1* functions as a molecular switch connecting the circadian clock with plant responses to drought. *EMBO Journal* **28**: 3745–3757.

Lenth R, Singmann H, Love J, Buerkner P, Herve M. 2018. *emmeans: estimated marginal means, aka least-squares means. R package v.1.2.3.* [WWW document] URL https://github.com/rvlenth/emmeans [accessed 12 April 2019].

Li R, Llorca LC, Schuman MC, Wang Y, Wang L, Joo Y, Wang M, Vassão DG, Baldwin IT. 2018. ZEITLUPE in the roots of wild tobacco regulates jasmonate-mediated nicotine biosynthesis and resistance to a generalist herbivore. *Plant Physiology* **177**: 833–846.

Li R, Wang M, Wang Y, Schuman MC, Weinhold A, Schäfer M, Jiménez-Alemán GH, Barthel A, Baldwin IT. 2017. Flower-specific jasmonate signaling regulates constitutive floral defenses in wild tobacco. *Proceedings of the National Academy of Sciences, USA* **114**: E7205–E7214.

Lynds GY, Baldwin IT. 1998. Fire, nitrogen, and defensive plasticity in *Nicotiana attenuata*. *Oecologia* **115**: 531–540.

Makino S, Matsushika A, Kojima M, Oda Y, Mizuno T. 2001. Light response of the circadian waves of the APRR1/TOC1 quintet: when does the quintet start singing rhythmically in Arabidopsis?. *Plant and Cell Physiology* **42**: 334–339.

Más P, Kim W-YY, Somers DE, Kay SA, Mas P, Kim W-YY, Somers DE, Kay SA. 2003. Targeted degradation of TOC1 by ZTL modulates circadian function in *Arabidopsis thaliana*. *Nature* **426**: 567–570.

Massad TJ, Dyer LA, Vega CG. 2012. Costs of defense and a test of the carbon-nutrient balance and growth-differentiation balance hypotheses for two co-occurring classes of plant defense. *PLoS ONE* **7**: e47554.

McCloud ES, Baldwin IT. 1997. Herbivory and caterpillar regurgitants amplify the wound-induced increases in jasmonic acid but not nicotine in *Nicotiana sylvestris*. *Planta* **203**: 430–435.

McGale E, Diezel C, Schuman MC, Baldwin IT. 2018. Cry1Ac production is costly for native plants attacked by non-Cry1Ac-targeted herbivores in the field. *New Phytologist* **219**: 714–727.

McKey D. 1974. Adaptive patterns in alkaloid physiology. *The American Naturalist* **108**: 305–320.

McKey D. 1979. The distribution of secondary compounds within plants. In: Rosenthal GA, Janzen DH, eds. *Herbivores: their interactions with secondary plant metabolites*. New York, NY, USA: Academic Press, 56–133.

Meldau S, Baldwin IT. 2013. Just in time: circadian defense patterns and the optimal defense hypothesis. *Plant Signaling & Behavior* **8**: e24410.

Meldau S, Erb M, Baldwin IT. 2012. Defence on demand: mechanisms behind optimal defence patterns. *Annals of Botany* **110**: 1503–1514.

Merchante C, Stepanova AN. 2017. The triple response assay and its use to characterize ethylene mutants in *Arabidopsis*. In: Binder B, Eric Schaller G, eds. *Ethylene signaling. Methods in molecular biology*, vol. **1573**. New York, NY, USA: Humana Press, 163–209.

Müller LM, Von Korff M, Davis SJ. 2014. Connections between circadian clocks and carbon metabolism reveal species-specific effects on growth control. *Journal of Experimental Botany* **65**: 2915–2923.

Nohales MA, Kay SA. 2016. Molecular mechanisms at the core of the plant circadian oscillator. *Nature Structural and Molecular Biology* **23**: 1061–1069.

Ohnmeiss TE, Baldwin IT. 1994. The allometry of nitrogen to growth and an inducible defense under nitrogen-limited growth. *Ecology* **75**: 995–1002.

Onkokesung N, Gaquerel E, Kotkar H, Kaur H, Baldwin IT, Galis I. 2012. MYB8 controls inducible phenolamide levels by activating three novel hydroxycinnamoyl-coenzyme A: polyamine transferases in *Nicotiana attenuata*. *Plant Physiology* **158**: 389–407.

R Core Team. 2018. *R: a language and environment for statistical computing*. Vienna, Austria: R Foundation for Statistical Computing. [WWW document] URL http://www.R-project.org/ [accessed 12 April 2019].

Rhoades DF. 1979. Evolution of plant chemical defenses against herbivores. In: Rosenthal GA, Janzen DH, eds. *Herbivores: their interactions with secondary plant metabolites*. New York, NY, USA: Academic Press, 3–54.

Rstudio Team. 2016. *RStudio: integrated development for R*. Boston, MA, USA: RStudio, PBC. [WWW document] URL http://www.rstudio.com/ [accessed 12 April 2019].

Sanchez SE, Kay SA. 2016. The plant circadian clock: from a simple timekeeper to a complex developmental manager. *Cold Spring Harbor Perspectives in Biology* **8**: a027748.

Sanchez-Villarreal A, Shin J, Bujdoso N, Obata T, Neumann U, Du SX, Ding Z, Davis AM, Shindo T, Schmelzer E *et al.* 2013. *TIME for COFFEE* is an essential component in the maintenance of metabolic homeostasis in *Arabidopsis thaliana*. *The Plant Journal* **76**: 188–200.

Schäfer M, Brütting C, Baldwin IT, Kallenbach M. 2016. High-throughput quantification of more than 100 primary- and secondary-metabolites, and phytohormones by a single solid-phase extraction based sample preparation with analysis by UHPLC–HESI–MS/MS. *Plant Methods* **12**. doi: 10.1186/s13007-016-0130-x

Schäfer M, Brütting C, Gase K, Reichelt M, Baldwin I, Meldau S. 2013. 'Real time' genetic manipulation: a new tool for ecological field studies. *The Plant Journal* **76**: 506–518.

Schuman MC, Baldwin IT. 2016. The layers of plant responses to insect herbivores. *Annual Review of Entomology* **61**: 373–394.

Seo PJ, Mas P. 2015. STRESSing the role of the plant circadian clock. *Trends in Plant Science* **20**: 230–237.

Sharma M, Bhatt D. 2015. The circadian clock and defence signalling in plants. *Molecular Plant Pathology* **16**: 210–218.

Sheard LB, Tan X, Mao H, Withers J, Ben-Nissan G, Hinds TR, Kobayashi Y, Hsu FF, Sharon M, Browse J *et al.* 2010. Jasmonate perception by inositol-phosphate-potentiated COI1-JAZ co-receptor. *Nature* **468**: 400–405.

Sherman PW. 1988. Levels of analysis. *Animal Behaviour* **36**: 616–619.

Shoji T, Kajikawa M, Hashimoto T. 2010. Clustered transcription factor genes regulate nicotine biosynthesis in tobacco. *Plant Cell* **22**: 3390–3409.

Shoji T, Nakajima K, Hashimoto T. 2000. Ethylene suppresses jasmonate-induced gene expression in nicotine biosynthesis. *Plant and Cell Physiology* **41**: 1072–1076.

Somers DE, Webb AAR, Pearson M, Kay SA. 1998. The short-period mutant, *toc1-1*, alters circadian clock regulation of multiple outputs throughout development in *Arabidopsis thaliana*. *Development* **125**: 485–494.

Song Q, Ando A, Xu D, Fang L, Zhang T, Huq E, Qiao H, Deng XW, Jeffrey Chen Z. 2018. Diurnal down-regulation of ethylene biosynthesis mediates biomass heterosis. *Proceedings of the National Academy of Sciences, USA* **115**: 5606–5611.

Soy J, Leivar P, González-Schain N, Martín G, Diaz C, Sentandreu M, Al-Sady B, Quail PH, Monte E. 2016. Molecular convergence of clock and photosensory pathways through PIF3–TOC1 interaction and co-occupancy of target promoters. *Proceedings of the National Academy of Sciences, USA* **113**: 4870–4875.

Stamp N. 2003. Out of the quagmire of plant defense hypotheses. *The Quarterly Review of Biology* **78**: 23–55.

Steppuhn A, Gase K, Krock B, Halitschke R, Baldwin IT. 2004. Nicotine's defensive function in nature. *PLoS Biology* **2**: e217.

Takase M, Mizoguchi T, Kozuka T, Tsukaya H. 2013. The unique function of the *Arabidopsis* circadian clock gene *PRR5* in the regulation of shade avoidance response. *Plant Signaling & Behavior* **8**: e23534.

Taubert M, Jehmlich N, Vogt C, Richnow HH, Schmidt F, von Bergen M, Seifert J. 2011. Time resolved protein-based stable isotope probing (Protein-SIP) analysis allows quantification of induced proteins in substrate shift experiments. *Proteomics* **11**: 2265–2274.

Thain SC, Vandenbussche F, Laarhoven LJJ, Dowson-Day MJ, Wang Z-Y, Tobin EM, Harren FJM, Millar AJ, Van Der Straeten D. 2004. Circadian rhythms of ethylene emission in *Arabidopsis*. *Plant Physiology* **136**: 3751–3761.

Thines B, Katsir L, Melotto M, Niu Y, Mandaokar A, Liu G, Nomura K, He SY, Howe GA, Browse J. 2007. JAZ repressor proteins are targets of the SCF (COI1) complex during jasmonate signalling. *Nature* **448**: 661–665.

Thorpe KW, Barbosa P. 1986. Effects of consumption of high and low nicotine tobacco by *Manduca sexta* (Lepidoptera: Sphingidae) on survival of gregarious endoparasitoid *Cotesia congregata* (Hymenoptera: Braconidae). *Journal of Chemical Ecology* **12**: 1329–1337.

Tinbergen N. 1963. On aims and methods of ethology. *Zeitschrift für Tierpsychologie* **20**: 410–433.

Ullmann-Zeunert L, Muck A, Wielsch N, Hufsky F, Stanton MA, Bartram S, Böcker S, Baldwin IT, Groten K, Svatoš A *et al.* 2012. Determination of ^{15}N-incorporation into plant proteins and their absolute quantitation: a new tool to study nitrogen flux dynamics and protein pool sizes elicited by plant–herbivore interactions. *Journal of Proteome Research* **11**: 4947–4960.

Ullmann-Zeunert L, Stanton MA, Wielsch N, Bartram S, Hummert C, Svatoš A, Baldwin IT, Groten K. 2013. Quantification of growth-defense trade-offs in a common currency: nitrogen required for phenolamide biosynthesis is not derived from ribulose-1,5-bisphosphate carboxylase/oxygenase turnover. *The Plant Journal* **75**: 417–429.

Valim HF, McGale E, Yon F, Halitschke R, Fragoso V, Schuman MC, Baldwin IT. 2019. The clock gene *TOC1* in shoots, not roots, determines fitness of *Nicotiana attenuata* under drought. *Plant Physiology* **181**: 305–318.

Voelckel C, Baldwin IT. 2004. Generalist and specialist lepidopteran larvae elicit different transcriptional responses in *Nicotiana attenuata*, which correlate with larval FAC profiles. *Ecology Letters* **7**: 770–775.

Voelckel C, Schittko U, Baldwin IT. 2001. Herbivore-induced ethylene burst reduces fitness costs of jasmonate and oral secretion-induced defenses in *Nicotiana attenuata*. *Oecologia* **127**: 274–280.

Von Dahl CC, Winz RA, Halitschke R, Kühnemann F, Gase K, Baldwin IT. 2007. Tuning the herbivore-induced ethylene burst: the role of transcript accumulation and ethylene perception in *Nicotiana attenuata*. *The Plant Journal* **51**: 293–307.

Wagner MR, Mitchell-Olds T. 2018. Plasticity of plant defense and its evolutionary implications in wild populations of *Boechera stricta*. *Evolution* **72**: 1034–1049.

Wang KLC, Li H, Ecker JR. 2002. Ethylene biosynthesis and signaling networks. *Plant Cell* **14**: 131–152.

Watkins CB. 2006. The use of 1-methylcyclopropene (1-MCP) on fruits and vegetables. *Biotechnology Advances* **24**: 389–409.

Winz RA, Baldwin IT. 2001. Molecular interactions between the specialist herbivore *Manduca sexta* (Lepidoptera, Sphingidae) and its natural host *Nicotiana attenuata*. IV. Insect-induced ethylene reduces jasmonate-induced nicotine accumulation by regulating putrescine N-methyltransfer. *Plant Physiology* **125**: 2189–2202.

Woldemariam MG, Dinh ST, Oh Y, Gaquerel E, Baldwin IT, Galis I. 2013. *NaMYC2* transcription factor regulates a subset of plant defense responses in *Nicotiana attenuata*. *BMC Plant Biology* **13**: 73.

Wu J, Baldwin IT. 2010. New insights into plant responses to the attack from insect herbivores. *Annual Review of Genetics* **44**: 1–24.

Yon F, Seo PJ, Ryu JY, Park C, Baldwin IT, Kim S-G. 2012. Identification and characterization of circadian clock genes in a native tobacco, *Nicotiana attenuata*. *BMC Plant Biology* **12**: 172.

Zangerl AR, Rutledge CE. 1996. The probability of attack and patterns of constitutive and induced defense: a test of optimal defense theory. *American Naturalist* **147**: 599–608.

Zhang C, Gao M, Seitz NC, Angel W, Hallworth A, Wiratan L, Darwish O, Alkharouf N, Dawit T, Lin D *et al.* 2019. *LUX ARRHYTHMO* mediates crosstalk between the circadian clock and defense in *Arabidopsis*. *Nature Communications* **10**: 1–14.

Zhu J-Y, Oh E, Wang T, Wang Z-Y. 2016. TOC1–PIF4 interaction mediates the circadian gating of thermoresponsive growth in Arabidopsis. *Nature Communications* **7**: 1–10.

Supporting Information

Additional Supporting Information may be found online in the Supporting Information section at the end of the article.

Fig. S1 Effect of *TOC1* silencing on whole-plant nicotine and phenolamide pools.

Fig. S2 Ethylene burst after elicitation with *Manduca sexta* oral secretions is not affected by whole-plant nor root-only *TOC1* silencing.

Fig. S3 Effect of *TOC1* silencing on transcript abundance of various ethylene receptors and downstream targets 1 h after simulated herbivory.

Fig. S4 Effect of silencing *NaTOC1* on ethylene triple response.

Fig. S5 Chlorogenic acid accumulation is attenuated in irTOC1 plants 72h after simulated herbivory.

Notes S1 Expanded statistical information and outlier removal.

Table S1 Primer sequences used in this study.

Please note: Wiley Blackwell are not responsible for the content or functionality of any Supporting Information supplied by the authors. Any queries (other than missing material) should be directed to the *New Phytologist* Central Office.